

The anthropogenic fallout radionuclides in soils of Mount Khuko (the Western Caucasus) and their application for determination of sediment redistribution

Maksim M. Ivanov^{a,b,*}, Natalia V. Kuzmenkova^{a,c}, Alexandra K. Rozhkova^c, Evgeniy A. Grabenko^a, Alexei M. Grachev^a, Valentin N. Golosov^{a,b}

^a Institute of Geography RAS, Russia

^b Faculty of Geography, Lomonosov Moscow State University, Russia

^c Faculty of Chemistry, Lomonosov Moscow State University, Russia

ARTICLE INFO

Keywords:

Cesium-137

Chernobyl

Nuclear bomb testing

^{239,240}Pu

Erosion

Sedimentation

ABSTRACT

The purposes of this study are to determine the content and origin of anthropogenic fallout radionuclides (FRN) in soils of Mount Khuko, located in the western sector of the Caucasus Mountains and to assess the possibility to use them for evaluation of sediment redistribution for the alpine grasslands.

The field study was carried out in August 2019 near the top of Mount Khuko, located in the western part of the main Caucasus Mountain Ridge. Integral and incremental soil samples were collected from the different morphological units of the studied area. The content of ¹³⁷Cs and ²⁴¹Am in soil samples was evaluated using laboratory gamma-spectrometry. A part of samples was selected for Pu isotopes extraction and then alpha-spectrometric analysis.

It was established that the ¹³⁷Cs contamination of soils in the studied area has at least two sources of origin. The first source is the ¹³⁷Cs bomb-derived fallout after the bomb tests in 1950–60th, which is widespread across the globe. The second source is ¹³⁷Cs Chernobyl-derived fallout. High random variability ($C_v = 25\text{--}42\%$) was found within reference sites, located at the undisturbed areas on the local flat interfluvies due to high variability of soil characteristics (grain size, density, organic matter content etc.). However minimum spatial variability (range 12.2–14.3 kBq/m²) was identified for the mean value of ¹³⁷Cs inventories for all 5 reference sites located in the different parts of the studied area. It is difficult to separate individual peaks of the bomb-derived and Chernobyl-derived ¹³⁷Cs fallout in sediment sinks with low sedimentation rates.

Application ^{239,240}Pu as an additional chronological marker allows to identify the origin of above mentioned peaks in the soils of alpine grasslands and of dry lake bottom.

1. Introduction

Technogenic fallout radionuclides (FRN), together with natural radionuclides ²¹⁰Pb_{ex} and ⁷Be, are widely used as tracers in sedimentation studies (Ritchie et al., 1974; Ritchie and McHenry, 1990; Zapata, 2003; Collins and Walling, 2004; Davis and Fox, 2009; Haddadchi et al., 2013; Golosov et al., 2018). The most successful for these purposes are those radionuclides that are firmly bound to soil particles. These include technogenic ¹³⁷Cs (Squire and Middleton, 1966; Adeleye et al., 1994; Von Gunten and Beneš, 1995; Efremov, 1988; Salbu, 2006, 2009;

Semenkova et al., 2018), various Pu and ²⁴¹Am isotopes (Sholkovitz, 1983; Livens and Baxter, 1988; Penrose et al., 1990; Clark, 2000; Hinton and Pinder, 2001; Choppin, 2007; Romanchuk et al., 2016). The correct application of radioisotope techniques is possible if there is confirmed information about the sources of their emissions, the spatial variability of the initial deposition and the characteristics of their behavior in the environment. This information is available for several regions (Lee et al., 1998; Zhang and Hou, 2019; Meusburger et al., 2020), and is also generalized for the entire globe (Kelley et al., 1999; Taylor, 2001). The use of ¹³⁷Cs as an tracer has proven to be extremely useful for assessing

* Corresponding author. Institute of Geography RAS, Russia.

E-mail addresses: ivanovm@bk.ru (M.M. Ivanov), kuzmenkova213@gmail.com (N.V. Kuzmenkova), rozhkovaak@gmail.com (A.K. Rozhkova), grabenko@inbox.ru (E.A. Grabenko), almgrachev@yandex.ru (A.M. Grachev), gollossov@gmail.com (V.N. Golosov).

<https://doi.org/10.1016/j.jenvrad.2022.106880>

Received 12 July 2021; Received in revised form 25 March 2022; Accepted 28 March 2022

0265-931X/© 2022 Elsevier Ltd. All rights reserved.

the rate of erosion and sedimentation, primarily in watersheds with a high proportion of arable land and grassland (Owens et al., 1997; Walling and He, 1997, 1999; Ritchie, 2000; Panin et al., 2001; Zapata, 2002; Hassan and Ergenzinger, 2003; Ritchie and Ritchie, 2005; Belyaev et al., 2009; Olson et al., 2013). There are various sources of origin for ^{137}Cs that have been identified for most of Europe, Japan and some other regions, including global fallout from nuclear bomb tests and regional and local radioactive accidents. The presence of ^{137}Cs of various origins in sediment makes it possible to estimate the intensity of sedimentation rates in different time windows based on the interpretation of the ^{137}Cs depth distribution curves (Golosov et al., 2018). Plutonium, and especially its isotopes $^{239,240}\text{Pu}$, has also been considered in recent years as one of the most promising long-lived radioactive tracers (Arata et al., 2016a,b; Alewell et al., 2017). The determination of ^{241}Am (a daughter radionuclide ^{241}Pu) is an alternative to radiocaesium dating, which allows the identification of the 1963 peak in the accumulative strata corresponding to the period of maximum bomb-derived fallout (Appleby et al., 1991; Arnaud et al., 2006; Oldfield et al., 1995; Arnaud et al., 2006; Appleby, 2002; Lusa et al., 2009; Corcho-Alvarado et al., 2014). High mountain systems, such as the Caucasus, acting as barriers to the migration of air masses (Barry, 1992; Efimov and Anisimov, 2011) leads to the formation of high precipitation on the windward slopes (Kononova, 2015; Tashilova et al., 2019), and intense and uneven accumulation of FRN in soil (Stewart et al., 1959; Lance et al., 1986; Bunzl and Kracke, 1988; UNSCEAR, 1993; Blagoeva and Zikovskiy, 1995; Wright et al., 1999; Kvasnikova et al., 1999). It is assumed that there are two sources of radionuclide inputs in Caucasus: bomb-derived fallout during nuclear weapons tests with a maximum fallout in 1963 (UNSCEAR, 1982; Hirose et al., 1987), and Chernobyl fallout from April–May 1986, (Izrael et al., 1996; De Cort, 1998). Contamination by technogenic radionuclides of the Caucasus and, in particular, its Northern macroslope remains insufficiently studied. It is reflected in a few publications, although in recent years there has been a certain increase in their number (Kordzadze et al., 2013; Buraeva et al., 2015; Kekelidze et al., 2017; Urushadze and Manakhov, 2017; Łokas et al., 2018; Kuzmenkova et al., 2020; Pyuskyulyan et al., 2020).

The study of the bottom sediments of the lake Khuko in the Western Caucasus revealed a high content of technogenic radionuclides. Due to extremely low rates of sedimentation, technogenic radionuclides were concentrated in the near-surface part of the 0.5 cm thick sedimentary strata (Kuzmenkova et al., 2020). It was assumed that the high concentration of ^{137}Cs was constituted after the Chernobyl accident. At the same time, the relatively high concentration of ^{241}Am is associated with the fallout of radionuclides during the nuclear bombs testing in the open atmosphere. A high concentration of $^{239,240}\text{Pu}$ was detected, which could potentially indicate some exotic source of radionuclides. However, an analysis of the $^{240}\text{Pu}/^{239}\text{Pu}$ isotopic ratio indicated bomb-derived fallout as the most likely source (Kuzmenkova et al., 2020).

A similar set of radionuclides and their concentrations have already been recorded earlier in cryoconites of the Agishi glacier in the central part of the Caucasus Range (Georgia) (Łokas et al., 2018). But in the given case, the main reason is a process of concentration of radioactive atmospheric aerosols on the surface of the glacier with the participation of microorganisms (cyanobacteria). For the conditions at Khuko Lake, there is no evidence that such a concentration mechanism takes place.

The purpose of this study is to determine the local variability of technogenic radionuclides in the soils of the Mount Khuko, and assessment of possibility of their use as tracers. Within the framework of this study, the following tasks were solved:

1. Determination of the ^{137}Cs fallout of the initial spatial variability in soils of the Mount Khuko at reference sites and comparing the obtained values with regional studies and available radioecological maps.

2. Conducting a field gamma-spectrometric survey for the evaluation of spatial distribution of the radionuclides within the different morphological units of the study area.
3. Investigation of the radionuclide (^{137}Cs , $^{239,240}\text{Pu}$ and ^{241}Am) depth distributions in the local sediment sinks and evaluation to possibilities to use them for evaluations of sedimentation rates for the different time windows.

2. Materials and methods

The study was carried out in the beginning of August 2019 on the top of the Mount Khuko, located in the western part of the main Caucasus Mountain Ridge (Fig. 1). The mountain is part of the watershed line between the Pshekhaskha (a tributary of the Pshekh River) and the Shakhe Rivers, and it is located 7 km northwest of Mount Fisht (highest top of the main Caucasus Ridge in the Western Caucasus). The summit of Mount Khuko Kh is located within the belt of alpine meadows. The upper border of the forest belt is located somewhat lower along the slopes.

Lake Khuko (see SM-1 A, C) has an area of 27,500 m² with a maximum depth of 10 m and a small catchment area (≈120,000 m²). It maintains a positive water balance due to intense precipitation (≈1500 mm year⁻¹) and a thick snow cover, which can persist until July (Efremov, 1988). Under the conditions of a general warming of the climate in the end of XX and first decades of XXI centuries, there are significant fluctuations in the annual precipitation with a slight increase in February–March and October–November (Aleshina et al., 2018). The topography of Mount Khuko is characterized by high complexity and may be subdivided into three morphological units: northwestern, central, and southeastern (see SM-1 A). The northwestern and central units were apparently a single system, starting from the Khuko Lake, which is currently isolated from the cascade of shallow lake-like depressions occupying the northern slope of the mountain (see SM-1 B). Currently, these lake-like depressions turn into swamps and gradually dry up. A large proportion of the northwestern part of the mountain and the catchment area of the Khuko Lake are covered with beech forest and shrubs adjacent to alpine grasslands.

The southeastern unit of the mountain top is represented by a ridge with relatively gentle northern and steep southern slopes. The northern slope is dissected by a series of shallow hollows that break the continuous herbaceous cover. Downstream they flow into the channel of a stream flowing down from the slope of the mountain. In the mouths of some hollows, there are traces of material accumulation in the form of proluvium fans with dense grass vegetation (see SM-1 D).

The soil cover is represented by light loamy soddy-calcareous leached soils of mountain meadows (Molchanov, 2010) with an average thickness of up to 40 cm (SM-2 A). In the lower part of the soil profile, the share of parent rock fragments, represented by limestones and marls, exceeds 50% (Kazeev et al., 2012). In deluvial sediments filling the bottom of hollows and sediments composing proluvium fans, The proportion of clay and sandy particles increases significantly in the sediments of the hollow bottoms and proluvium fans (see SM-2 B).

2.1. Sampling procedure

5 relatively flat undisturbed locations were selected as a reference sites for evaluation of the initial spatial variability of ^{137}Cs fallout. (see Fig. 2). Soil samples were taken at five points on each reference locations. Samples were taken in the corners of a square with sides of 2.5–3.0 m and the point of intersection of its diagonals. The sections with depths maximum 30–40 cm were dug in the each sampling locations. In some cases, a bedrock matter was excavated (see SM-2 A). Samples were cut from the front wall of the section. The size of the each sample was 10 × 10 × 10 cm in size. It was assumed that a depth of 10 cm is sufficient for the evaluation of the total inventory of radionuclides.

Two areas were identified, where it was expected both erosion and deposition processes during the last decades. The first area is



Fig. 1. Location of Mount Khuko on the map of radioactive contamination of Europe with ^{137}Cs (bomb-derived and Chernobyl-derived) (Izrael et al., 1996).

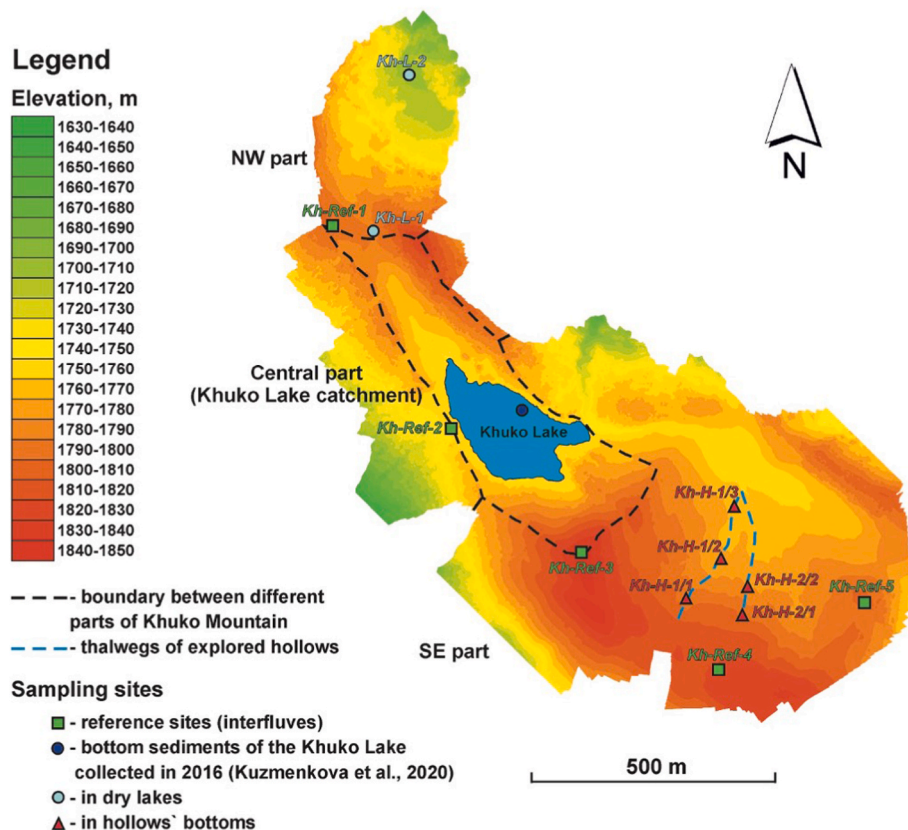


Fig. 2. Topography and sampling sites location at the studied area (the Mount Khuko).

represented by the bottoms of hollows and proluvium fans in the southeastern morphological unit (Fig. 2, SM-1 D). They are clearly distinguished in the relief in the form of depressions with a flat bottom and smooth elevations up to 1 m in height in the lower parts. They are also well labeled with thicker, more moisture-loving grass vegetation (see SM-3). The second area is represented by the bottoms of drying lake-like depressions in the northwestern part of the study area (Fig. 2, SM-1 B). Totally, two cores were collected at the bottoms of dry lakes and five cores were collected at the bottoms and fans of the hollows (Fig. 2). Depth increment sampling was carried out in areas of expected sedimentation using a metal sampler with an internal diameter of 3 cm (see SM-4 A, B). Samples were cut into 1 cm thick sections directly inside

the sampler. After that, each of the samples was packed in separate plastic bags, and the sampler was cleaned using wet wipes.

2.2. Field gamma-spectrometry survey

The field gamma-spectrometric survey was undertaken at the top area of the Khuko lake using a detector with a 63×63 mm NaI (TI) crystal packed in an aluminum case 80 mm in diameter and a resolution of at least 6.3%. The spectrometer was placed in backpack on the height of 1 m above the ground. The measurement error count rate of registration of ^{137}Cs in the measurements points (CPS) consists of two: the error of the initial calibration (when the new activity was converted to

cps) and the statistical. The error was estimated as 20% for the investigated points during the moving. A GPS receiver was connected to the detector, and the AtomSpectraGPS software was used. The exposure time was from 10 to 15 min, depending on the counting rate (see SM-4 C). The peak of the registration intensity of gamma quanta in the region of 661.7 keV was clearly visible in each of the spectra obtained in the field (see SM-5).

2.3. Laboratory analysis

At the initial stage rocks and particles bigger than 2 mm were separated from the sample using a set of sieves. The samples were dried in an oven at a temperature of 105 °C. Bulk density was assessed. Further samples were crashed, and were packed in containers with a fixed cylindric geometry for subsequent gamma spectrometric analysis. Determination of the gamma-active radionuclides content was carried out using an ORTEC GEM-C5060P4-B gamma spectrometer using ultrapure germanium (HPGe) semiconductor detector with a beryllium window, and relative efficiency of 20%. The detection efficiency of ^{137}Cs (661.7 keV) - 2.5% (1–3 g samples) and 1.5% (30–100 g samples), ^{241}Am (59.3 keV) - 18% (1–3 g samples) and 7% (30–100 g samples). The exposure time of the samples was from 60 000 to 250 000 s, depending on the observed intensity of registration of the desired radionuclides. Sample weights with fixed geometry ranged from 1 to 3 g for the samples sliced in sampler and 30–100 g for samples taken in soil section within reference sites. The minimum detected activity (MDA) for ^{137}Cs isotopes was 0.06 Bq for the reference sites samples, and 0.5 Bq for the core samples.

Two cores with contrasting vertical distribution of ^{137}Cs were selected for the determination of Pu isotopes via alpha spectrometry: one core from hollow and one from dry lake. Before the extraction samples were ashed (450 °C, 8 h). A sample weighing 1 g was investigated. Complete acid decomposition was carried out by sequential addition of concentrated hydrofluoric acid, a mixture of HF:HNO₃ in a ratio of 3:1, dry boric acid in a mixture with concentrated hydrochloric acid, and concentrated nitric acid with the addition of 30% H₂O₂. After each stage, the resulting solution with the test sample was evaporated to wet salts. Obtained wet salts were dissolved in 7.5M HNO₃. For the extraction of plutonium anionite grade AB-17 × 8 was used. The crystalline NaNO₂ was added to the target solution for stabilization the isotopes of plutonium in Pu(IV). The solution was heated for 5 min at a temperature of 100 °C and kept until the release of brown vapor ceased (this step speeds up the nitrite decomposition reaction). The resulting solution was passed through a column with a previously prepared resin, then the column was sequentially washed with 7.5M HNO₃, 9M HCl, 7.5M HNO₃, and distilled water. Plutonium isotopes were separated by washing off the anionite with hydrochloric acid hydroxylamine heated to 40 °C, then precipitated from the resulting solution with cerium fluorides. To control the radiochemical yield, 10 µL of ^{236}Pu with an activity of 0.2 Bq was added to the ashed sample. The preparation of counting samples consisted of co-precipitation of plutonium with CeF₃ on a Resolve filter (Methods developed by Eichrom Technologies LLC). The analysis of the content of alpha-emitting radionuclides (^{238}Pu , $^{239,240}\text{Pu}$) was carried out on an ORTEC Alfa-Esemble-2 alpha spectrometer with an ENS-U900 with silicon detector (UL-TRA-AS). The minimum detected activity (MDA) for Pu isotopes was 0.05 Bq.

3. Results

3.1. ^{137}Cs inventories at the reference sites

Examination of samples taken at the reference sites recorded relatively high level of the ^{137}Cs fallout. The average level of soil contamination of the Mount Khuko, estimated at 5 points, varies in the range of 12.2–14.3 kBq m⁻², which is quite consistent with the data of the published map of initial radioactive contamination of European Russia

(Fig. 1), where the density of surface soil contamination in the study area ranges from 10 to 40 kBq m⁻² (Izrael et al., 1996; De Cort, 1998). High local spatial variability of ^{137}Cs was identified within each of five reference sites. It is largely due to the high proportion of coarse material (coarser than sand) in shallow soils. The average coefficients of variation (CV) were relatively high for the all reference locations (42%: Kh-Ref-1 - 34%, Kh-Ref-2 - 25%, Kh-Ref-3 - 43%, Kh-Ref-4 - 45%, Kh-Ref-5 - 63%). (Table 1).

3.2. Results of filed gamma-spectrometric survey

The presence of significant ^{137}Cs concentrations in the soil of the studied area was also confirmed by the conducted field gamma-spectrometric survey (Fig. 3).

The points with obtained values of input count rate (counts per second – CSP) were subdivided into groups based on the previously mentioned morphological units: into the northwestern, central, and southeastern parts of the studied area.

The lack of correlation between measurement point elevation and input count rate (CPS) was detected for the northwestern and central morphological units of Mount Khuko (Fig. 4 A, B). Such a result is generally expected for conditions with high variability of the soil grain size and low rates of erosion and sedimentation, which is indirectly confirmed by the very low sedimentation rate in the Khuko lake (Kuzmenkova et al., 2020).

For the south-eastern morphological unit, where clear geomorphological signs of erosion and sediment redeposition were found, a weak inverse correlation between elevation and input count rate (CPS) was revealed. This fact may indicate an increase in ^{137}Cs deposits along with the sedimentation of eroded soil particles at lower positions. When considering the above dependencies, it is worth taking into account the previously described heterogeneity of ^{137}Cs deposition on the soil

Table 1
Some characteristics of samples taken at the reference locations (the leached soddy-calcareous soils of alpine meadows).

Reference site	Sampling point	Bulk density, kg m ⁻³	Proportion, %		^{137}Cs deposits, kBq m ⁻²
			Silt, sand, organic matter	Gravel, boulders	
Kh-Ref-1	1	410	100	0	19.9 ± 0.2
	2	300	100	0	11.5 ± 0.1
	3	188	100	0	10.9 ± 0.1
	4	228	100	0	9.6 ± 0.2
	5	490	87	13	10.1 ± 0.1
Kh-Ref-2	mean	323	97	3	12.4 ± 6.4
	1	718	100	0	15.6 ± 0.1
	2	560	100	0	14.2 ± 0.2
	3	676	79	21	12.9 ± 0.2
	4	634	100	0	7.9 ± 0.1
Kh-Ref-3	5	594	100	0	10.5 ± 0.1
	mean	636	96	4	12.2 ± 6.7
	1	196	100	0	9.6 ± 0.1
	2	287	70	30	19.7 ± 0.5
	3	448	100	0	8.6 ± 0.1
Kh-Ref-4	4	208	100	0	18.2 ± 0.1
	5	250	100	0	8.3 ± 0.1
	mean	278	94	6	12.9 ± 8.2
	1	508	100	0	16.8 ± 0.2
	2	489	100	0	9.9 ± 0.1
Kh-Ref-5	3	591	87	13	7.5 ± 0.3
	4	573	100	0	19.9 ± 0.3
	5	338	100	0	8.1 ± 0.1
	mean	500	97	3	12.4 ± 7.1
	1	629	100	0	24.2 ± 0.2
Kh-Ref-5	2	718	100	0	10.7 ± 0.2
	3	502	100	0	23.6 ± 0.2
	4	332	100	0	6.5 ± 0.1
	5	393	88	12	6.5 ± 0.1
	mean	515	98	2	14.3 ± 7.7

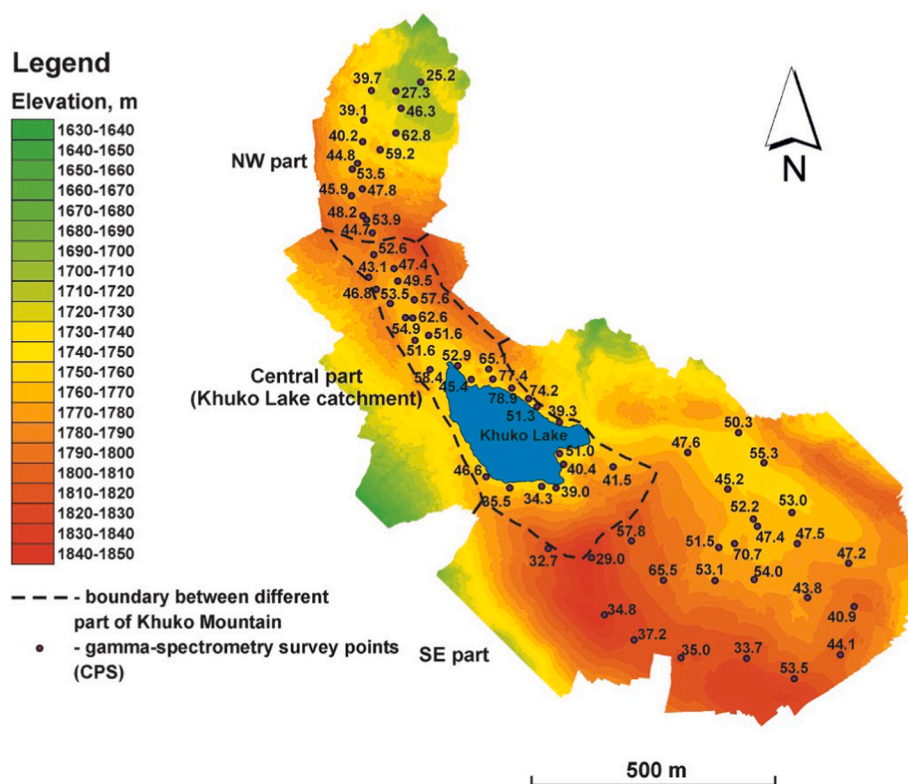


Fig. 3. Input count rate of registration of ^{137}Cs (CPS) in the measurement points of the different parts (morphological units) of the studied area (Mount Khuko).

surface to avoid incorrect interpretations. Nevertheless, the obtained correlation indirectly justifies the choice of a site for sampling layer-by-layer samples at the tops of proluvium fans.

3.3. ^{137}Cs depth distribution interpretation

The ^{137}Cs depth distributions at the bottoms of the two studied hollows are presented in Tables 2 and 3. In the case of the hollow Kh-H-1, all three collected cores showed different types of ^{137}Cs depth distribution (Table 2). The core Kh-H-1/1 was the only example that contains two separate maximums of ^{137}Cs inventory at depths of 0–1 and 4–5 cm. It can be assumed that the upper maximum associated with Chernobyl-derived ^{137}Cs fallout in May 1986. In this case, the maximum content of ^{137}Cs at a depth of 4–5 cm should be attributed to maximum of bomb-derived ^{137}Cs fallout in 1963. However, this assumption seems to be erroneous, since in this case, the pre-Chernobyl ^{137}Cs inventory should be of the order of 16 kBq m^{-2} . This is too high for bomb-derived fallout. In addition, the insignificant ^{137}Cs inventory in the 1–2 cm layer compared to the ^{137}Cs deposits in the upper and lower layers allows to suggest that the peak at a depth of 4–5 cm is more likely associated with the Chernobyl fallout in May 1986. In this case, the relatively high ^{137}Cs concentration in the surface layer can be associated with a washout from the catchment area of the hollow.

The location of maximum of ^{137}Cs inventory in the layer 1–2 cm indicate the lack of sediment deposition in central part of hollow bottom (core Kh-H-1/2). It is the most likely overlap of the peaks of bomb-derived and Chernobyl fallout in the given sampling point. The such situation is typical for areas with high levels of Chernobyl fallout (Golosov, 2002).

^{137}Cs depth distribution is relatively uniform from the surface to the 10 cm depth in the core Kh-H-1/3, located at the proluvium fan (Table 2). Such a ^{137}Cs depth distribution indicates that this is sediments redeposited during post-Chernobyl period. The option with a possible erosion of the Chernobyl peak seems unlikely, due to the low gradient of the surface and the dispersion of runoff within the fan. Therefore, the

accumulation of material carried out from the catchment areas of the hollows most likely led to the burial of the surface exposed at the moment of the Chernobyl fallout, and the sampling depth was insufficient for the evaluation of the location of the ^{137}Cs inventory maximum associated with Chernobyl fallout.

The depth distributions of ^{137}Cs in sediments of the bottom of the hollow Kh-H-2 (Table 3) are different. Total deposits of ^{137}Cs in Kh-H-2/2 are three times higher than in Kh-H-2/1, which may be explained by uneven erosion and redeposition of sediments along the hollow's bottom. At the same time, two peaks of cesium reserves were found in Kh-H-2/2, unlike a single one in Kh-H-2/1, which is very similar to the difference in depth distributions seen in the bottom of the first hollow.

In the bottoms of the two drying up lakes, the upper 10 cm is represented by organogenic deposits with a maximum of ^{137}Cs deposits at a depth of 3–4 cm (Table 4). Such a distribution turns out to be quite expected. It is clearly indicating the very low input of the sediment from the catchment area, and hence a low rate of sedimentation, which mainly associated with dead plant residues.

3.4. Vertical distribution of $^{239,240}\text{Pu}$ deposits and $^{239,240}\text{Pu}/^{137}\text{Cs}$ ratio in samples taken from the hollow (Kh-H-1/1) and dry lake (Kh-L-2)

Radiochemical extraction of Pu was performed for two cores with the most contrasting ^{137}Cs distribution. The core Kh-H-1/1 was selected first due to the presence of two distinct maximums of ^{137}Cs deposits, both of which were proposed to have ^{137}Cs of Chernobyl origin, and the determination of Pu in these samples helped to test this hypothesis. The second studied core was Kh-L-2. The main goal was to separate the ^{137}Cs deposits of bomb-derived and Chernobyl-derived origin in the context of low sedimentation rates and the possible overlapping of the both ^{137}Cs peaks. In each of the selected cores, the Pu isotope radiochemical extraction procedure was performed for the top 6 samples. In all samples, only $^{239,240}\text{Pu}$ isotopes were reliably detected, as in the study of bottom sediments of Lake Khuko. Plutonium isotopes ^{241}Pu and ^{238}Pu were not detected. (Kuzmenkova et al., 2020) (Table 5).

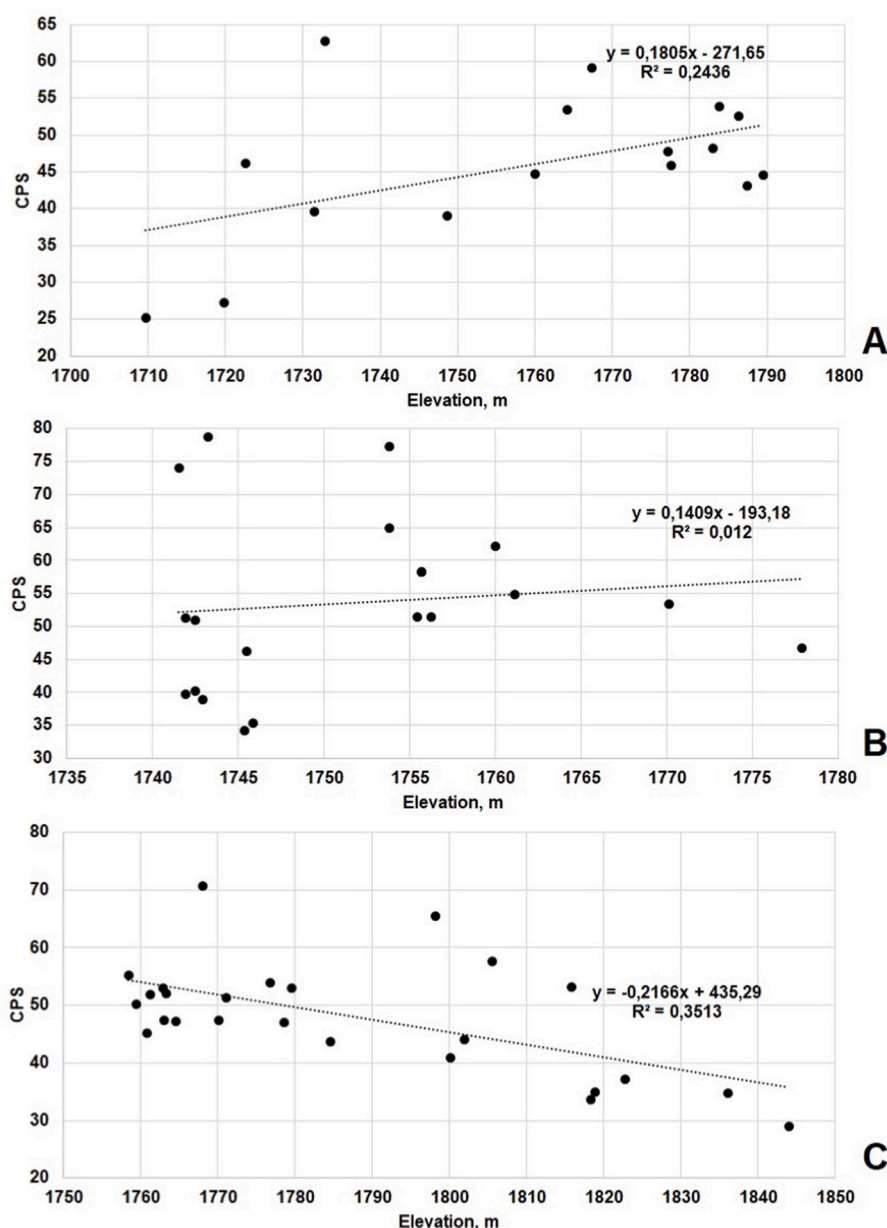


Fig. 4. Dependencies between elevation of the sampling points and obtained CPS values for different morphological units of Mount Khuko: A – NW part, B – central part, C – SE part.

In the core Kh-H-1/1, there is an unsystematic distribution of $^{239,240}\text{Pu}$ deposits with a high variability – in the upper 5 cm layer (CV – 50%). At the same time, the $^{239,240}\text{Pu}/^{137}\text{Cs}$ ratio turns out to be typical for the Chernobyl fallout, which confirms the hypothesis that deposits up to 4 cm accumulated over the post-Chernobyl period, and the peak of the Chernobyl ^{137}Cs fallout is located at a depth of 4–5 cm. There is an increase in the $^{239,240}\text{Pu}/^{137}\text{Cs}$ ratio in the sample collected from the depth of 6–7 cm. It indicates a likely greater contribution of bomb-derived fallout to the formation of ^{137}Cs deposits.

The clear maximum of $^{239,240}\text{Pu}$ was recorded at a depth of 3–4 cm in the core Kh-L-2, where the largest ^{137}Cs inventory was also observed. On the whole, such distribution does not contradict the situation of overlapping bomb-derived and Chernobyl-derived peaks, given that the overlying layer with a low concentration of $^{239,240}\text{Pu}$ contain more than half of the total ^{137}Cs inventory in the core. The $^{239,240}\text{Pu}/^{137}\text{Cs}$ ratios with the maximum values in the lower part of the section confirm this explanation. In general, a trend with an increase in the $^{239,240}\text{Pu}/^{137}\text{Cs}$

ratio with depth in the soils was previously noted for mountain catchments (Meusburger et al., 2018), where radioactive contamination was associated with bomb-derived and Chernobyl-derived fallouts (Alewell et al., 2014).

^{241}Am was detected in samples but unfortunately, the uncertainty was too high to make quantitative analysis (more than 45%). Hence, investigation of americium content requires radiochemical extraction, which is planned to conduct in the future.

4. Discussion

Obtained results indicate that the ^{137}Cs contamination of the soils of Mount Khuko has a complex origin with the contribution of at least two documented sources of FRN, namely: bomb-derived fallout after bomb tests in the 1950–60th and the Chernobyl accident. Intensive deposition of FRN in soils of Mount Khuko was most likely due to high precipitation on the windward slopes of the Caucasus Mountains, which is a favorable

Table 2¹³⁷Cs vertical distribution in cores taken from the hollow Kh-H-1.

Kh-H-1/1 (bottom)			Kh-H-1/2 (bottom)			Kh-H-1/3 (proluvium fan)		
Depth, cm	¹³⁷ Cs		Depth, cm	¹³⁷ Cs		Depth, cm	¹³⁷ Cs	
	Deposits, kBq m ⁻²	Specific activity, Bq kg ⁻¹		Deposits, kBq m ⁻²	Specific activity, Bq kg ⁻¹		Deposits, kBq m ⁻²	Specific activity, Bq kg ⁻¹
0–1	7.08 ± 0.14^a	3163 ± 47	0–1	5.93 ± 0.18	9379 ± 281	0–1	0.92 ± 0.07	587 ± 47
1–2	1.07 ± 0.08	667 ± 47	1–2	10.6 ± 0.21	7428 ± 149	1–2	1.04 ± 0.08	585 ± 47
2–3	3.23 ± 0.07	1579 ± 32	2–3	4.25 ± 0.13	2325 ± 70	2–3	2.02 ± 0.08	598 ± 24
3–4	3.50 ± 0.14	1236 ± 49	3–4	2.05 ± 0.06	760 ± 23	3–4	2.75 ± 0.11	513 ± 21
4–5	4.25 ± 0.13	1547 ± 46	4–5	1.34 ± 0.07	423 ± 21	4–5	1.99 ± 0.06	484 ± 15
5–6	2.03 ± 0.10	606 ± 30	5–6	0.57 ± 0.05	182 ± 15	5–6	2.05 ± 0.08	409 ± 16
6–7	1.09 ± 0.07	233 ± 14	6–7	0.47 ± 0.05	90 ± 9	6–7	1.52 ± 0.08	372 ± 19
7–8	0.47 ± 0.06	67 ± 8	7–8	0.18 ± 0.03	57 ± 10	7–8	1.70 ± 0.09	384 ± 19
8–9	0.37 ± 0.04	44 ± 5	8–9	0.23 ± 0.04	46 ± 8	8–9	2.12 ± 0.09	369 ± 15
9–10	0.30 ± 0.04	49 ± 7	9–10	0.16 ± 0.03	27 ± 6	9–10	2.15 ± 0.11	345 ± 17
Total	23.4 ± 0.87	–	Total	25.8 ± 0.85	–	Total	18.26 ± 0.85	–

^a Layers with maximum ¹³⁷Cs inventory are pointed with bold font.**Table 3**Vertical distribution of ¹³⁷Cs in cores from the hollow Kh-H-2.

Kh-H-2/1(bottom)			Kh-H-2/2 (bottom)		
Depth, cm	¹³⁷ Cs		Depth, cm	¹³⁷ Cs	
	Deposits, kBq m ⁻²	Specific activity, Bq kg ⁻¹		Deposits, kBq m ⁻²	Specific activity, Bq kg ⁻¹
0–1	0.43 ± 0.05	918 ± 101	0–1	4.61 ± 0.23	3878 ± 194
1–2	0.87 ± 0.06	1022 ± 72	1–2	2.69 ± 0.11	3537 ± 141
2–3	2.09 ± 0.08^a	982 ± 39	2–3	4.42 ± 0.18	4458 ± 134
3–4	2.00 ± 0.08	717 ± 29	3–4	4.61 ± 0.21	4128 ± 206
4–5	0.65 ± 0.05	196 ± 16	4–5	2.55 ± 0.15	2010 ± 121
5–6	0.33 ± 0.04	79 ± 9	5–6	2.52 ± 0.15	2009 ± 121
6–7	0.24 ± 0.02	63 ± 5	6–7	1.5 ± 0.05	1369 ± 41
7–8	0.16 ± 0.02	60 ± 8	7–8	0.74 ± 0.07	764 ± 69
8–9	0.06 ± 0.02	20 ± 7	8–9	0.54 ± 0.05	442 ± 40
9–10	0.08 ± 0.02	17 ± 4	9–10	0.13 ± 0.01	107 ± 11
Total	6.91 ± 0.44	–	Total	24.32 ± 1.21	–

^a Layers with maximum ¹³⁷Cs deposits are pointed with bold font.

condition for the fallout of bomb (UNSCEAR, 1993) and Chernobyl origin (Kvasnikova et al., 1999) radionuclides. This situation is quite typical for the mountainous areas of Europe: the Alps, Massif Central, the Ardennes, and the Rhine Mountains (Meusburger et al., 2020). The presence of two sources at different times implies the possibility of determining sedimentation rates over different periods second half of the XX and the beginning of the XXI centuries. Two different peaks of ¹³⁷Cs content may be attributed to the moment of fallouts associated with the maximum fallout of radionuclides during the period of nuclear tests, which in the northern hemisphere took place in 1963, and Chernobyl fallout in the period from late April to May 1986. Under the conditions of the climate change in the Caucasus region (Toropov et al., 2019) and subsequent changes in the environment (Solomina et al., 2015, 2016), the possibility of using radioisotope methods to assess the rate of sedimentation is crucial to obtain information about environmental feedback on climatic changes (Kuzmenkova et al., 2020; Grachev et al., 2020). However, the sampling and subsequent interpretation of the depth distribution of radionuclides should be taken into account

Table 4Vertical distribution of ¹³⁷Cs inventory in cores taken from dry lake bottoms.

Kh-L-1			Kh-L-2		
Depth, cm	¹³⁷ Cs		Depth, cm	¹³⁷ Cs	
	Deposits, kBq m ⁻²	Specific activity, Bq kg ⁻¹		Deposits, kBq m ⁻²	Specific activity, Bq kg ⁻¹
0–2*	1.13 ± 0.06	792 ± 40	0–1	0.79 ± 0.02	941 ± 57
			1–2	1.23 ± 0.09	1085 ± 54
2–3	1.12 ± 0.07	991 ± 59	2–3	1.93 ± 0.04	1468 ± 73
3–4	1.56 ± 0.08	2191 ± 110	3–4	2.54 ± 0.10	1509 ± 60
4–5	3.48 ± 0.10	2137 ± 64	4–5	0.89 ± 0.03	357 ± 25
5–6	2.60 ± 0.10	1506 ± 60	5–6	0.28 ± 0.01	141 ± 17
6–7	0.78 ± 0.06	415 ± 29	6–7	0.14 ± 0.03	43 ± 8
7–8	0.35 ± 0.04	181 ± 22	7–8	0.09 ± 0.03	31 ± 10
8–9	0.20 ± 0.03	98 ± 16	8–9	0.07 ± 0.02	20 ± 5
9–10	0.19 ± 0.03	70 ± 11	9–10	0.09 ± 0.02	19 ± 5
Total	11.41 ± 0.57	–	Total	8.05 ± 0.39	–

*a large number of plant roots did not allow to accurately divide this layer into intervals of 0–1 and 1–2 cm.

with serious constraints.

Relatively low rates of sedimentation, the step size of depth incremental sampling may be too big to isolate deposits of various origins due to their possible overlapping, as was revealed in the majority of observed cores. Under conditions when the level of Chernobyl contamination significantly exceeds bomb-derived fallout, the overlapping process is quite typical (Golosov, 2002). Based on the available radioecological maps and results of the our observations described above, we can conclude that within the study area, the largest part of ¹³⁷Cs inventories was associated with the Chernobyl fallout. Nevertheless, in some points, the ratio of radionuclide fallout of different origin can vary greatly due to the peculiarities of sediment lateral migration. As it was found for the soils of Mount Aragat in the monitoring zone of the Armenian NPP, located outside the area with relatively high level of Chernobyl contamination, ¹³⁷Cs inventory may reach values of 10.5–11.47 kBq m⁻² (Pyuskyulyan et al., 2020). This is very close to the level of radioactive contamination of the soils of Mount Khuko. At the

Table 5

Vertical distribution of $^{239,240}\text{Pu}$ inventory and $^{239,240}\text{Pu}/^{137}\text{Cs}$ ratio in samples from the cores Kh-H-1/1, Kh-L-2 and expected sources of ^{137}Cs deposits.

Depth, cm	^{239,240} Pu		^{239,240} Pu/ ¹³⁷ Cs (1988) ^a	Source of ¹³⁷ Cs fallout ^b
	deposits, Bq m ⁻²	Specific activity, Bq kg ⁻¹		
Kh H-1/1 (hollow)				
0–1	21.3 ± 0.9	9.5 ± 0.4	0.001 ± 0.0001	Chernobyl
1–2	15.2 ± 1	8.6 ± 0.6	0.007 ± 0.001	Chernobyl
2–3	26.6 ± 1.2	12.8 ± 0.6	0.004 ± 0.0003	Chernobyl
3–4	48.4 ± 2.1	17.1 ± 0.7	0.007 ± 0.001	Chernobyl
4–5	19.7 ± 0.9	7.2 ± 0.3	0.002 ± 0.0002	Chernobyl
5–6	sample is lost			
6–7	29.3 ± 1.3	6.3 ± 0.3	0.013 ± 0.001	Chernobyl, Global
Total ^c	131 ± 5.8	–	0.003 ± 0.0002	Chernobyl
Kh-L-2 (lake)				
0–1	18.5 ± 0.9	22.1 ± 1.1	0.011 ± 0.001	Chernobyl ^d
1–2	2.4 ± 0.1	2.1 ± 0.1	0.001 ± 0.0001	Chernobyl
2–3	20.5 ± 1	15.6 ± 0.8	0.005 ± 0.0004	Chernobyl
3–4	160 ± 8	95 ± 4.8	0.031 ± 0.003	Global
4–5	56.1 ± 3	23.7 ± 1.3	0.032 ± 0.003	Global
5–6	50.7 ± 2.5	25.2 ± 1.2	0.087 ± 0.009	Global
Total	311 ± 15.5	–	0.02 ± 0.002	Chernobyl, Global
Lake Khuko (Kuzmenkova et al., 2020)				
0–0.5			0,027 ± 0003	Chernobyl, Global

^a values are recalculated to 1988 for comparison published data.

^b threshold values for detection of ^{137}Cs source were taken from Kuzmenkova et al. (2020) и Meusburger et al. (2020): Chernobyl <0.008; Chernobyl, Global 0.008–0.029; Global >0.029.

^c only upper 5 cm

^d according to the depth of sampling, performed isotope ratio may be assumed as possible for Chernobyl fallout.

same time, on the territory of Georgia, such a high level of radioactive contamination of at least arable soils was observed only on the Black Sea coast and it was not recorded in the eastern high-mountainous regions (Urushadze and Manakhov, 2017), located on the possible migration pathways of air masses between the Chernobyl nuclear power plant and Mount Aragat. Participation of exotic sources of radionuclides is unlikely. However, the results of the study of cryoconite in the central part of the Caucasus mountains to the probability of some undocumented sources of radionuclide contamination of the given region (Lokas et al., 2018). The most likely explanation for the occurrence of such high values with an average density of bomb-derived ^{137}Cs fallouts in the northern hemisphere of 3.42 kBq m⁻² (UNSCEAR, 1982) may be the concentration of the finely dispersed fraction of sediments eroded from the slopes, in which the most intense fixation of radionuclides is observed.

If this process takes place, then the formation of peaks of ^{137}Cs deposits is possibly caused not by direct fallout, but by sorting of material during erosion and redeposition. Such an explanation in the presence of Chernobyl contamination is quite consistent with the observed distribution in cores Kh-H-1/1 and Kh-H-1/3. In the case of Kh-H-1/1 and Kh-H-2/2, the maximum deposits in the near-surface layer could have been formed by a local source of thin and highly radioactive material. In core Kh-H-1/3, the “Chernobyl peak” was not identified at all, either due to erosion, or insufficient sampling depth or due to both of these reasons at the same time. Moreover, in the sediments accumulated already after 1986, there is no clear trend towards a decrease in the ^{137}Cs content, which is not typical for catchments in Chernobyl affected areas (Konoplev et al., 2020). The unevenness of the participation of local sources in the formation of slope sediment runoff turns out to overcome the process of mixing and averaging the concentration of radionuclides in the material during transportation.

Based on the foregoing, it follows that a situation may arise in which

an unambiguous interpretation of the vertical distribution with clearly pronounced peaks of ^{137}Cs deposits, becomes difficult without the use of additional time markers. In the absence of disturbance, the peak of $^{239,240}\text{Pu}$ inventory can be used as an additional chronomarker (Lal et al., 2013), although the process of its determination by alpha or mass spectrometry is much more laborious in comparison with gamma spectrometry. This marker can be even more reliable than ^{137}Cs , due to the possibility of determining its origin by isotopic ratios. The high variability of $^{239,240}\text{Pu}$ deposits in the Kh-H-1/1 core indicates a nonlinear increase in deposits during sedimentation. Assuming the absence of a significant input of Pu isotopes from the atmosphere, it may indicate the uneven participation of various sources in the formation of slope sediment runoff within relatively compact areas. In this regard, the application of models that use Pu stock changes to assess erosion and sediment accumulation (Meusburger et al., 2018; Arata et al., 2016a;b) should be carried out with a statistically reliable set of field data that allows for local variability of the initial radionuclide fallout.

5. Conclusion

The soils of the alpine belt of the Western Caucasus are contaminated by bomb-derived and Chernobyl-derived ^{137}Cs . This makes it possible to estimate the sedimentation rates over two time windows.

High spatial variability of the ^{137}Cs initial deposition was revealed for the reference sites located in the zone of alpine meadows in the Western Caucasus. This is due to the high unevenness of various characteristics (density, texture, grain size etc.) of thin soils in this altitudinal belt. At the same time, the average ^{137}Cs inventory at the five surveyed reference sites within the study area are quite close, varying in the range from 12 to 14 kBq m⁻².

The relationship between the elevation of the area and the content of ^{137}Cs was established only for the morphological unit with traces of erosion-accumulative processes clearly expressed in the relief.

Assessment of the ^{137}Cs depth distribution in the sediment sinks (bottom of hollows, proluvial cones and bottoms of dry lakes) made it possible to determine the rates of modern accumulation, which reached maximum values in the proluvial fan. However, only the use of $^{239+240}\text{Pu}$ as an additional chronomarker made it possible to reliably separate the sediments deposited in the post-Chernobyl period and for the period 1963–1986 in areas with low accumulation rates.

Declaration of competing interest

The authors declare that they have no known competing financial interests or personal relationships that could have appeared to influence the work reported in this paper.

Acknowledgments

The work was conducted with financial support from the ongoing Russian Science Foundation project No. 19-17-00181: “Quantitative assessment of the slope sediment flux and its changes in the Holocene for the Caucasus mountain rivers.” This study contributes to the State Task no. FMGE- FMGE-2019–0005, Institute of Geography RAS.

Appendix A. Supplementary data

Supplementary data to this article can be found online at <https://doi.org/10.1016/j.jenvrad.2022.106880>.

References

- Adeleye, S.A., Clay, P.G., Oladipo, M.O.A., 1994. Sorption of caesium, strontium and europium ions on clay minerals. *J. Mater. Sci.* 29 (4), 954–958.
- Aleshina, M.A., Toropov, P.A., Semenov, V.A., 2018. Temperature and humidity regime changes on the Black Sea coast in 1982–2014. *Russ. Meteorol. Hydrol.* 43 (4), 235–244.

- Alewell, C., Meusburger, K., Juretzko, G., Mabit, L., Ketterer, M.E., 2014. Suitability of $^{239+240}\text{Pu}$ and ^{137}Cs as tracers for soil erosion assessment in mountain grasslands. *Chemosphere* 103, 274–280.
- Alewell, C., Pitols, A., Meusburger, K., Ketterer, M., Mabit, L., 2017. $^{239+240}\text{Pu}$ from “contaminant” to soil erosion tracer: where do we stand? *Earth Sci. Rev.* 172, 107–123.
- Appleby, P.G., Richardson, N., Nolan, P.J., 1991. ^{241}Am dating of lake sediments. *Hydrobiologia* 214 (1), 35–42.
- Appleby, P.G., 2002. Chronostratigraphic techniques in recent sediments. In: *Tracking Environmental Change Using Lake Sediments*. Springer, Dordrecht, pp. 171–203.
- Arata, L., Alewell, C., Frenkel, E., A'Campo-Neuen, A., Iurian, A.-R., Ketterer, M.E., et al., 2016a. Modelling deposition and erosion rates with RadioNuclides (MODERN) – part 2: a comparison of different models to convert $^{239+240}\text{Pu}$ inventories into soil redistribution rates at unploughed sites. *J. Environ. Radioact.* 162–163, 97–106.
- Arata, L., Meusburger, K., Frenkel, E., A'Campo-Neuen, A., Iurian, A.-R., Ketterer, M.E., et al., 2016b. Modelling deposition and erosion rates with RadioNuclides (MODERN) – part 1: a new conversion model to derive soil redistribution rates from inventories of fall-out radionuclides. *J. Environ. Radioact.* 162–163, 45–55.
- Arnaud, F., Magand, O., Chapron, E., Bertrand, S., Boës, X., Charlet, F., Mélières, M.A., 2006. Radionuclide dating (^{210}Pb , ^{137}Cs , ^{241}Am) of recent lake sediments in a highly active geodynamic setting (Lakes Puyehue and Icalma—Chilean Lake District). *Sci. Total Environ.* 366 (2–3), 837–850.
- Barry, R.G., 1992. *Mountain Weather and Climate*. Psychology Press, p. 244.
- Belyaev, V.R., Golosov, V.N., Kuznetsova, J.S., Markelov, M.V., 2009. Quantitative assessment of effectiveness of soil conservation measures using a combination of ^{137}Cs radioactive tracer and conventional techniques. *Catena* 79, 214–227.
- Blagoeva, R., Zikovskiy, L., 1995. Geographic and vertical distribution of Cs-137 in soils in Canada. *J. Environ. Radioact.* 27 (3), 269–274.
- Bunzl, K., Kracke, W., 1988. Cumulative deposition of ^{137}Cs , ^{238}Pu , $^{239+240}\text{Pu}$ and ^{241}Am from global fallout in soils from forest, grassland and arable land in Bavaria (FRG). *J. Environ. Radioact.* 8 (1), 1–14.
- Buraeva, E.A., Bezuglova, O.S., Stasov, V.V., Nefedov, V.S., Dergacheva, E.V., Goncharenko, A.A., Martynenko, S.V., Goncharov, L.Yu., Gorbov, S.N., Malyshevskiy, V.S., Vardun, T.V., 2015. Features of ^{137}Cs distribution and dynamics in the main soils of the steppe zone in the southern European Russia. *Geoderma* 259, 259–270.
- Choppin, G., 2007. Actinide speciation in the environment. *J. Radioanal. Nucl. Chem.* 273 (3), 695–703.
- Clark, D.L., 2000. The chemical complexities of plutonium. *Los Alamos Sci.* 26, 364–381.
- Collins, A.L., Walling, D.E., 2004. Documenting catchment suspended sediment sources: problems, approaches and prospects. *Prog. Phys. Geogr.* 28 (2), 159–196.
- Corcho-Alvarado, J.A., Diaz-Asencio, M., Froidevaux, P., Bochud, F., Alonso-Hernández, C.M., Sanchez-Cabeza, J.A., 2014. Dating young Holocene coastal sediments in tropical regions: use of fallout $^{239,240}\text{Pu}$ as alternative chronostratigraphic marker. *Quat. Geochronol.* 22, 1–10.
- De Cort, M., 1998. Atlas of Caesium Deposition on Europe after the Chernobyl Accident.
- Davis, C.M., Fox, J.F., 2009. Sediment fingerprinting: review of the method and future improvements for allocating nonpoint source pollution. *J. Environ. Eng.* 135 (7), 490–504.
- Efimov, V.V., Anisimov, A.E., 2011. Climatic parameters of wind-field variability in the Black Sea region: numerical reanalysis of regional atmospheric circulation. *Izvestiya Atmos. Ocean. Phys.* 47 (3), 350–361.
- Eremov, Yu. V., 1988. Goluboe ozerel'e Kavkaza (*Blue Necklace of the Caucasus*) (In Russian). Gidrometeoizdat, Leningrad, pp. 89–92.
- Golosov, V.N., 2002. Special considerations for areas affected by Chernobyl fallout. In: Zapata, F. (Ed.), *Handbook for the Assessment of Soil Erosion and Sedimentation Using Environmental Radionuclides*, vol. 1. Kluwer Academic Publishers, Dordrecht, The Netherlands, pp. 165–184.
- Golosov, V.N., Walling, D.E., Konoplev, A.V., Ivanov, M.M., Sharifullin, A.G., 2018. Application of bomb-and Chernobyl-derived radiocaesium for reconstructing changes in erosion rates and sediment fluxes from croplands in areas of European Russia with different levels of Chernobyl fallout. *J. Environ. Radioact.* 186, 78.
- Grachev, A.M., Novenko, E.Y., Grabenko, E.A., Alexandrin, M.Y., Zazovskaya, E.P., Konstantinov, E.A., et al., 2020. The Holocene Paleoenvironmental History of Western Caucasus (Russia) Reconstructed by Multi-Proxy Analysis of the Continuous Sediment Sequence from Lake Khuko. The Holocene, 0959683620972782.
- Haddadchi, A., Ryder, D.S., Evrard, O., Olley, J., 2013. Sediment fingerprinting in fluvial systems: review of tracers, sediment sources and mixing models. *Int. J. Sediment Res.* 28 (4), 560–578.
- Hassan, M.A., Ergenzinger, P., 2003. Use of tracers in fluvial geomorphology. *Tools Fluvial Geomorphol.* 397–423.
- Hinton, T.G., Pinder III, J.E., 2001. A review of plutonium releases from the Savannah River Site, subsequent behavior within terrestrial and aquatic environments and resulting dose to humans. *Radioact. Environ.* 1, 413–435.
- Hirose, K., Aoyama, M., Katsuragi, Y., Sugimura, Y., 1987. Annual deposition of Sr-90, Cs-137 and Pu-239,240 from the 1961-1980 nuclear explosions: a simple model. *J. Meteorol. Soc. Jpn. Ser. II* 65 (2), 259–277.
- Izrael, Yu A., Cort, M De, Jones, A.R., Nazarov, I.M., Fridman, Sh D., Kvasnikova, E.V., Stukin, E.D., Kelly, G.N., Matveenko, I.I., Pokumeiko Yu, M., Tabatchnyi, L Ya, Tsaturov, 1996. Yu. The Atlas of Cesium-137 Contamination of Europe after the Chernobyl Accident. Belarus: N.
- Kazeev, K.S., Kutrovskii, M.A., Dadenko, E.V., Vezdeneeva, L.S., Kolesnikov, S.I., Val'kov, V.F., 2012. The influence of carbonates in parent rocks on the biological properties of mountain soils of the Northwest Caucasus region. *Eurasian Soil Sci.* 45 (3), 282–289.
- Kekelidze, N., Jakhutashvili, T., Tutberidze, B., Tulashvili, E., Akhalkatsishvili, M., Mtsariashvili, L., 2017. Radioactivity of soils in Mtskheta-Mtianeti region (Georgia). *Ann. Agrar. Sci.* 15 (3), 304–311.
- Kelley, J.M., Bond, L.A., Beasley, T.M., 1999. Global distribution of Pu isotopes and ^{237}Np . *Sci. Total Environ.* 237, 483–500.
- Kononova, N.K., 2015. Changes in the northern hemisphere atmospheric circulation in the 20th–21st century and their consequences for climate. *Fundamental'naja i prikladnaja klimatologija* 1, 127–156 (In Russian).
- Konoplev, A., Kato, K., Kalmykov, S.N. (Eds.), 2020. Behavior of Radionuclides in the Environment II: Chernobyl. Springer Nature.
- Kordzadze, A.A., Surmava, A.A., Kukhalashvili, V.G., 2013. Numerical investigation of the air possible pollution in case of large hypothetical accidents in some industrial territories of the Caucasus. *J. Georgian Geophys. Soc.* 16, 13–23.
- Kvasnikova, E.V., Stukin, E.D., Golosov, V.N., 1999. Heterogeneity of ^{137}Cs contamination in an area at a large distance from the Chernobyl NPP. *Meteorologija i gidrologija* 3, 5–12.
- Kuzmenkova, N.V., Ivanov, M.M., Alexandrin, M.Y., Grachev, A.M., Rozhkova, A.K., Zhizhin, K.D., Grabenko, E.A., Golosov, V.N., 2020. Use of natural and artificial radionuclides to determine the sedimentation rates in two North Caucasus lakes. *Environ. Pollut.* 114269.
- Lal, R., Tims, S.G., Fifield, L.K., Wasson, R.J., Howe, D., 2013. Applicability of Pu-239 as a tracer for soil erosion in the wet-dry tropics of northern Australia. *Nucl. Instrum. Methods Phys. Res. Sect. B Beam Interact. Mater. Atoms* 294, 577–583.
- Lance, J.C., McIntyre, S.C., Naney, J.W., Rousseva, S.S., 1986. Measuring sediment movement at low erosion rates using cesium-137. *Soil Sci. Soc. Am. J.* 50 (5), 1303–1309.
- Lee, M.H., Lee, C.W., Boo, B.H., 1998. Distribution and characteristics of $^{239,240}\text{Pu}$ and ^{137}Cs in the soil of Korea. *J. Environ. Radioact.* 37 (1), 1–16.
- Livens, F.R., Baxter, M.S., 1988. Chemical associations of artificial radionuclides in Cumbrian soils. *J. Environ. Radioact.* 7 (1), 75–86.
- Lokas, E., Zawierucha, K., Cwanek, A., Szufa, K., Gaca, P., Mietelski, J.W., Tomankiewicz, E., 2018. The sources of high airborne radioactivity in cryoconite holes from the Caucasus (Georgia). *Sci. Rep.* 8 (1), 1–10.
- Lusa, M., Lehto, J., Leskinen, A., Jaakkola, T., 2009. ^{137}Cs , $^{239,240}\text{Pu}$ and ^{241}Am in bottom sediments and surface water of Lake Päijänne, Finland. *J. Environ. Radioact.* 100 (6), 468–476.
- Meusburger, K., Porto, P., Mabit, L., La Spada, C., Arata, L., Alewell, C., 2018. Excess Lead-210 and Plutonium-239+240: two suitable radiogenic soil erosion tracers for mountain grassland sites. *Environ. Res.* 160, 195–202.
- Meusburger, K., Evrard, O., Alewell, C., Borrelli, P., Cinelli, G., Ketterer, M., Mabit, L., Panagos, P., van Oost, K., Ballabio, C., 2020. Plutonium aided reconstruction of caesium atmospheric fallout in European topsoils. *Sci. Rep.* 10 (1), 1–16.
- Molchanov, E.N., 2010. Mountain-meadow soils of the highlands in the western Caucasus. *Eurasian Soil Sci.* 43 (12), 1330–1343.
- Oldfield, F., Richardson, N., Appleby, P.G., 1995. Radiometric dating (^{210}Pb , ^{137}Cs , ^{241}Am) of recent ombrotrophic peat accumulation and evidence for changes in mass balance. *Holocene* 5 (2), 141–148.
- Olson, K.R., Gennadiyev, A.N., Zhidkin, A.P., Markelov, M.V., Golosov, V.N., Lang, J.M., 2013. Use of magnetic tracer and radio-cesium methods to determine past cropland soil erosion amounts and rates. *Catena* 104, 103–110.
- Owens, P.N., Walling, D.E., He, Q., Shanahan, J.O., Foster, I.D., 1997. The use of caesium-137 measurements to establish a sediment budget for the Start catchment, Devon, UK. *Hydrol. Sci. J.* 42 (3), 405–423.
- Penrose, W.R., Polzer, W.L., Essington, E.H., Nelson, D.M., Orlandini, K.A., 1990. Mobility of plutonium and americium through a shallow aquifer in a semiarid region. *Environ. Sci. Technol.* 24 (2), 228–234.
- Pyuskiyulyan, K., La Mont, S.P., Atoyán, V., Belyaeva, O., Movsisyan, N., Saghatelian, A., 2020. Altitude-dependent distribution of ^{137}Cs in the environment: a case study of Aragats massif, Armenia. *Acta Geochimica* 39 (1), 127–138.
- Ritchie, J.C., Spraberry, J.A., McHenry, J.R., 1974. Estimating soil erosion from the redistribution of fallout ^{137}Cs . *Soil Sci. Soc. Am. J.* 38 (1), 137–139.
- Ritchie, J.C., McHenry, J.R., 1990. Application of radioactive fallout cesium-137 for measuring soil erosion and sediment accumulation rates and patterns: a review. *J. Environ. Qual.* 19 (2), 215–233.
- Ritchie, J.C., 2000. Combining ^{137}Cs and topographic surveys for measuring soil erosion/deposition patterns in a rapidly accreting area. *Acta Geol. Hisp.* 35 (3–4), 207–212.
- Ritchie, J.C., Ritchie, C.A., 2005. Bibliography of Publications of $^{137}\text{Cesium}$ Studies Related to Erosion and Sediment Deposition. USDA-ARS Hydrology and Remote Sensing Laboratory Occasional. Paper HRSL-2005-01.
- Romanchuk, A.Y., Kalmykov, S.N., Kersting, A.B., Zavarin, M., 2016. Behaviour of plutonium in the environment. *Russ. Chem. Rev.* 85 (9), 995.
- Salbu, B., 2006. Speciation of Radionuclides in the Environment. *Encyclopedia of Analytical Chemistry: Applications, Theory and Instrumentation*.
- Salbu, B., 2009. Fractionation of radionuclide species in the environment. *J. Environ. Radioact.* 100, 283–289.
- Semenkova, A.S., Evsiunina, M.V., Verma, P.K., Mohapatra, P.K., Petrov, V.G., Seregina, I.F., Bolshov, M.A., Krupskaya, V.V., Yu, Romanchuk A., Kalmykov, S.N., 2018. Cs+ sorption onto Kutch clays: influence of competing ions. *Appl. Clay Sci.* 166, 88–93.
- Sholkovitz, E.R., 1983. The geochemistry of plutonium in fresh and marine water environments. *Earth Sci. Rev.* 19 (2), 95–161.
- Solomina, O.N., Bradley, R.S., Hodgson, D.A., Ivy-Ochs, S., Jomelli, V., Mackintosh, A.N., et al., 2015. Holocene glacier fluctuations. *Quat. Sci. Rev.* 111, 9–34.
- Solomina, O.N., Bradley, R.S., Jomelli, V., Geirsdottir, A., Kaufman, D.S., Koch, J., et al., 2016. Glacier fluctuations during the past 2000 years. *Quat. Sci. Rev.* 149, 61–90.

- Squire, H.M., Middleton, L.J., 1966. Behaviour of Cs137 in soils and pastures a long term experiment. *Radiat. Bot.* 6 (5), 413–423.
- Stewart, N.G., Osmond, R.G., Crooks, R.N., Fisher, E.M., Owers, M.J., 1959. The Deposition Of Long-Lived Fission Products From Nuclear Test Explosions. Results up to the Middle of 1958 (No. AERE-Hp/r-2790). United Kingdom Atomic Energy Authority. Research Group. Atomic Energy Research Establishment, Harwell, Berks, England.
- Tashilova, A.A., Ashabokov, B.A., Kesheva, L.A., Teunova, N.V., 2019. Analysis of climate change in the Caucasus region: end of the 20th–beginning of the 21st century. *Climate* 7 (1), 11.
- Taylor, D.M., 2001. Environmental plutonium—creation of the universe to twenty-first century mankind. *Radioact. Environ.* 1, 1–14 (Elsevier).
- Toropov, P.A., Aleshina, M.A., Grachev, A.M., 2019. Large-scale climatic factors driving glacier recession in the Greater Caucasus, 20th–21st century. *Int. J. Climatol.* 39 (12), 4703–4720. <https://doi.org/10.1002/joc.6101>.
- Urushadze, T.F., Manakhov, D.V., 2017. Radioactive contamination of the soils of Georgia. *Ann. Agrar. Sci.* 15 (3), 375–379.
- UNSCEAR, 1982. Ionizing Radiation: Sources and Biological Effects. United Nations Scientific Committee on the Effects of Atomic Radiation, New York, p. 773.
- UNSCEAR, 1993. Report to the General Assembly, with Scientific Annexes. United Nations, New York).
- Von Gunten, H.R., Benes, P., 1995. Speciation of radionuclides in the environment. *Radiochim. Acta* 69 (1), 1–30.
- Walling, D.E., He, Q., 1997. Use of fallout ^{137}Cs in investigations of overbank sediment deposition on river floodplains. *Catena* 29 (3–4), 263–282.
- Walling, D.E., He, Q., 1999. Improved models for estimating soil erosion rates from ^{137}Cs measurements. *J. Environ. Qual.* 28, 611–622.
- Wright, S.M., Howard, B.J., Strand, P., Nylén, T., Sickel, M.A.K., 1999. Prediction of ^{137}Cs deposition from atmospheric nuclear weapons tests within the Arctic. *Environ. Pollut.* 104 (1), 131–143.
- Zapata, F. (Ed.), 2002. Handbook for the Assessment of Soil Erosion and Sedimentation Using Environmental Radionuclides. Kluwer Ac. Publ., Dordrecht, The Netherlands, p. 219.
- Zapata, F., 2003. The use of environmental radionuclides as tracers in soil erosion and sedimentation investigations: recent advances and future developments. *Soil Tillage Res.* 69 (1–2), 3–13.
- Zhang, W., Hou, X., 2019. Level, distribution and sources of plutonium in the coastal areas of China. *Chemosphere* 230, 587–595.